



Delft University of Technology

## Microgrid planning based on fuzzy interval prediction models of renewable resources

Morales, R.; Sáez , D.; Marín, L.G.; Nunez, Alfredo

**DOI**

[10.1109/FUZZ-IEEE.2016.7737706](https://doi.org/10.1109/FUZZ-IEEE.2016.7737706)

**Publication date**

2016

**Document Version**

Accepted author manuscript

**Published in**

2016 IEEE International Conference on Fuzzy Systems (FUZZ-IEEE)

**Citation (APA)**

Morales, R., Sáez , D., Marín, L. G., & Nunez, A. (2016). Microgrid planning based on fuzzy interval prediction models of renewable resources. In O. Cordon (Ed.), *2016 IEEE International Conference on Fuzzy Systems (FUZZ-IEEE): Vancouver, Canada* (pp. 336-343). IEEE. <https://doi.org/10.1109/FUZZ-IEEE.2016.7737706>

**Important note**

To cite this publication, please use the final published version (if applicable).

Please check the document version above.

**Copyright**

Other than for strictly personal use, it is not permitted to download, forward or distribute the text or part of it, without the consent of the author(s) and/or copyright holder(s), unless the work is under an open content license such as Creative Commons.

**Takedown policy**

Please contact us and provide details if you believe this document breaches copyrights.  
We will remove access to the work immediately and investigate your claim.

# Microgrid Planning based on Fuzzy Interval Models of Renewable Resources

R. Morales, D. Sáez, L. G. Marín

Department of Electrical Engineering  
University of Chile  
Santiago, Chile  
ramorale@ing.uchile.cl, dsaez@ing.uchile.cl,  
luis.marin@ing.uchile.cl

A. Nuñez

Railway Engineering Section  
Delft University of Technology  
Delft, Netherlands  
A.A.NunezVicencio@tudelft.nl

**Abstract**— Microgrids are sustainable solutions for electrification of rural zones that can make use of their local renewable resources. In this paper, we propose a new method for microgrid planning which includes the effect of the uncertainties of the renewable resources explicitly. Fuzzy interval models are used because they can capture nonlinearities and systematically represent the uncertainties associated with renewable resources at a certain confidence level. Relying on interval fuzzy models and by considering a set of possible scenarios for the renewable resources, the solution to the microgrid planning problem is given through the optimal sizing and topology of the microgrid. This information, particularly the optimal sizes of generators and the economic analysis, is useful for the design phase of a microgrid project. The proposed methodology is applied to the microgrid planning of the rural Mapuche community, José Painecura, in Chile.

**Keywords**— *microgrids; planning; fuzzy modelling.*

## I. INTRODUCTION

Access to electricity in rural areas is crucial for the development of local communities. The most relevant benefits are poverty reduction, lower risk of rural to urban migration, and improved quality of life, among others. Access to electricity together with well-designed sustainability plans can improve the quality and access to basic services like health and education, and can also facilitate the initiation of various local productive developments [1], [2]. In Latin America, governments have contributed to improving the standards of electricity supply in remote areas through national and regional electrification programs. However, most of these projects are extensions of the conventional electrical grid, which makes reaching every remote rural area and isolated community difficult because of the high costs of implementation, operation, and serious technical difficulties [3]. Moreover, in the case of communities with minority ethnic groups, special consideration should be taken to protect their distinct characteristics, to implement projects that are in agreement with their invaluable knowledge, beliefs and practices, and, particularly, to enlist their sustainable and collective management of their natural resources.

In this paper, the incorporation of Non-Conventional Renewable Energies (NCRE) as source of energy supply is

evaluated as a sustainable solution for electrification of rural areas [4]. The economic costs of operating NCRE projects can be lower than those of other types of traditional electrification projects. Additionally, the use of local renewable resources generates a lower environmental impact and contributes to global sustainability [2], [5]. These NCRE technologies, operating together with other micro-sources and loads, constitute a controllable low voltage system which is called a microgrid (MG) [6]. In countries like Denmark, the Netherlands, the United States, Japan, Canada, and Spain, there has been extensive experience installing MGs in urban areas [7]. For the electrification of rural areas, projects have been reported in Ecuador, South Africa, Morocco, and Bangladesh [8]. There are also special cases of MGs on islands, such as those implemented in Greece, Ecuador, and Mexico [7], [9].

The aim of this work, is to systematize the feasibility studies and planning of MG implementation projects for isolated rural communities.

Because of the high variability of wind and solar resources, models that include uncertainty are necessary. The fuzzy interval outputs correspond to the expected value and its variability, which represent all the possible trajectories of the renewable resources within a certain confidence level. The authors in [10], [11], and [12], presented the planning of MGs including the uncertainty of renewable resources and load. In [10], the authors introduced the microgrid planning model considering not only uncertainty in the load, but variable renewable generation, market prices, and the uncertainty associated with the isolated operation of the MG. Robust optimization is proposed for analyzing the worst-case solution of the planning. Planning that includes uncertainty modelling would increase optimal microgrid operation. In [11], the microgrid planning problem is defined, and anticipated interactions between the microgrid, the coupled microgrid, and the utility grid during grid-connected and islanded modes are considered. Robust optimization is used to visualize physical and financial uncertainties efficiently in the planning problem. In [12], the authors presented a multi-objective stochastic optimal planning method, and a stochastic chance-

constrained programming model to achieve economic and environmental benefits for the stand-alone microgrid. The uncertainties of wind speed, the clearness index, and load demand are considered based on the Markov process transition probability matrix.

Computational intelligence methods (IC) have been used to derive models of non-conventional renewable resources and load, due to their capacity to represent nonlinear systems [13]–[16]. Interval models are used to quantify the uncertainty associated with the renewable sources and load in [17]–[20]. The authors in [17] presented prediction intervals for the loads, applying the delta technique for constructing the intervals based on neural network models. In [18], the neuronal network model is used for the construction of the interval for the load and wind. And in [19] and [20], the authors presented fuzzy interval models for the renewable resources and load, using various methods for their construction.

The main contribution of this paper is the use of fuzzy interval models for microgrid planning. The fuzzy intervals permit including the uncertainties associated with the renewable resources, so that more realistic scenarios of renewable generation can be evaluated.

This paper is divided as follows: In Section II the microgrid planning problem and the fuzzy interval modelling approach are presented. In Section III, the solar and wind resource conditions for community are modelled with fuzzy intervals. Section IV contains an analysis of the optimal size of all the elements of the microgrid in regard to the cost function. Finally, conclusions and directions for further research are presented in Section V.

## II. PROPOSED FUZZY METHOD FOR MICROGRID PLANNING

### A. Microgrid Planning

At the start of a microgrid (MG) project, a careful planning process ensures the future optimal operation of the MG. The operation, in general, should perform optimally in all its objectives: economic, technical, and environmental [4], [10], [21]. Planning, the economic feasibility of MG implementation is investigated in this paper. The goal is to determine the optimal combination of distributed energy resources (DERs) to be installed in the MG, to guarantee the economic feasibility of the project.

It is possible to consider either a deterministic or a stochastic optimization approach in the MG design. In the deterministic approach, one considers average dynamics or a single realization of the stochasticities (one typical scenario). However, the performance will be guaranteed only for that selected scenario, making the MG design quite conservative and not optimal for a broad range of other instances. In the stochastic approach, the uncertainty of the demand and the renewable energy resources (which are inherently stochastic) are included explicitly in the optimization. This approach can guarantee good performance under a broader set of realizations

of the stochasticities, such as different days, and variations in the solar irradiance and wind speed.

The MG considered in this case study, is one that is connected intermittently to the main network. The natural resources available are accessed by means of photovoltaic arrays (PV) and wind turbines (W). A bank of batteries (BB) and a genset (GS) are also included. In this study, an optimal combination of MG components is found to satisfy the required electrical load, and optimize the least total Present Value of the Cost (PVC) [4]. The total PVC includes the initial capital cost of the components, the cost of the operation and maintenance (O&M), and the cost of component replacements that occur within the lifecycle of the project. It is necessary in the planning stage to size the different power generators accurately to meet the demand of the community with reliable and economical operation of the MG. Thus, the optimization planning problem is:

$$\min_{\{SoC_0, I_m, P_{m,y,d,h}\}} PVC_{PV} + PVC_W + PVC_{BB} + PVC_{GS} + PVC_{Grid}, \quad (1)$$

The decision variables are  $SoC_0$ ,  $I_m$  and  $P_{m,y,d,h}$ . The  $SoC_0$  is the initial state of the charge of the battery bank,  $I_m$  is the installed power [kW] for the generation unit  $m$ , and  $P_{m,y,d,h}$  is the instantaneous power [kW] for the generation unit  $m$  at the specific year  $y$ , day  $d$ , and hour  $h$ . Note that  $m$  stands for the generation unit and belongs to the set  $m \in \{PV, W, GS, BB, Grid\}$ .

The cost of investment in the main grid is assumed to be zero because the distribution network has already been installed. The cost of operation and maintenance of the main grid is given by the marginal energy cost (MEC), which is the amount that users pay to the electricity service provider. The Net Metering law is applied for the interchange of power between the MG and the main network.

The microgrid planning should also comply with a set of constraints. The first constraint applies to the balance of power, where the sum of the power generated by the photovoltaic array, the wind generator, battery bank, diesel generator and main grid must be equal to the power demand of the community  $P_{L,y,d,h}$  at each specified time (year, day, hour):

$$P_{L,y,d,h} = P_{PV,y,d,h} + P_{W,y,d,h} + P_{BB,y,d,h} + P_{GS,y,d,h} + P_{Grid,y,d,h} \quad (2)$$

The following constraints are related to the renewable resources. The power of the PV to satisfy the following constraint:

$$P_{PV,y,d,h} = \eta A_p G_{y,d,h}, \quad (3)$$

where  $\eta$  is the efficiency coefficient,  $A_p$  the covering area of the photovoltaic array [ $m^2$ ], and  $G_{y,d,h}$  is the solar irradiance at the specified time step year, day, hour in [ $W/m^2$ ].

The wind power is a function of the wind speed [m/s] ( $w_{y,d,h}$ ) at the specified time step (year, day, hour):

$$P_{w,y,d,h} = F(w_{y,d,h}) \quad (4)$$

The instantaneous power of each generating unit at a specified time should be less or equal to the installed capacity in the MG:

$$0 \leq P_{m,y,d,h} \leq I_m \quad m \in \{PV, w, GS, grid\} \quad (5)$$

In regard to the bank of batteries, the instantaneous power is given by the technology to be used. A minimum and maximum value of the state of the charge, which also depends on the technology used, must also be considered:

$$-P_{BB,\min} \leq P_{BB,y,d,h} \leq P_{BB,\max} = I_{BB} \quad (6)$$

$$SoC_{BB}^{\min} \leq SoC_{BB,y,d,h} \leq SoC_{BB}^{\max} \quad (7)$$

Finally, the Marginal Energy Cost (MEC) must be less than or equal to the current MEC. This is the value that the users pay to the service provider:

$$0 \leq MEC \leq MEC_{current} \quad (8)$$

In this paper, the uncertainties of the renewable energy resources (Photovoltaic and Wind) are included via Takagi-Sugeno interval fuzzy models, which capture the nonlinearities and stochasticities of the solar irradiation and the wind speed. The fuzzy interval modelling approach is described below.

### B. Fuzzy Interval Modelling

Takagi and Sugeno (T&S) described a type of fuzzy model that is suitable for approximating a large class of non-linear systems in [22]. The premises are based on fuzzy sets, and the consequences are local linear models that represent different operating points of the system. The T&S fuzzy models can be represented by the following expression:

$$\hat{y}(k) = \sum_{j=1}^{M_{TS}} \beta_j(x_p(k)) x^T(k) \theta_j, \quad (9)$$

where  $M_{TS}$  denotes the number of rules,  $x_p(k)$  and  $x^T(k)$  denote the vector of the premises and the consequences at time step  $k$ ,  $\beta_j(x_p(k))$  denotes the normalized activation degree of the  $j$ th rule, and  $\theta_j$  is the vector of parameters of the local linear model associated with the  $j$ th rule. For the normalized activation degree:

$$0 \leq \beta_j(x_p(k)) \leq 1, \quad j = 1, \dots, M_{TS} \quad (10)$$

$$\sum_{j=1}^{M_{TS}} \beta_j(x_p(k)) = 1 \quad (11)$$

In matrix form, the T&S model is represented as [23]:

$$\hat{y}(k) = \psi^T \Theta, \quad (12)$$

where  $\psi^T$  is the fuzzy regression matrix and  $\Theta$  is the matrix of coefficients for the whole set of rules, which are defined as:

$$\psi_j^T = \beta_j(x_p(k)) x^T(k) \quad (13)$$

$$\psi^T = [\psi_1^T, \dots, \psi_{M_{TS}}^T] \quad (14)$$

$$\Theta^T = [\theta_1, \dots, \theta_{M_{TS}}] \quad (15)$$

In this work, the identification procedure is divided in two parts. The fuzzy clustering method, which minimizes the number of rules, and generates the optimal fuzzy sets and rules via projections, is used for the identification of the premise parameters. The consequence parameters are obtained using the identification method based on least squares [24].

The uncertainty of the solar irradiance and wind speed are modeled using fuzzy confidence intervals. The intervals represent, with a certain confidence level, the regions where the trajectories of the wind speed and the solar irradiance are located. In other words, the fuzzy confidence interval defines a band that contains the measurement values with a certain confidence probability. In the design of fuzzy confidence interval models, one needs to find the upper bound fuzzy model  $\bar{f}(z(k))$  and the lower bound fuzzy model  $\underline{f}(z(k))$ . Based on [23], the analytical derivation of fuzzy confidence intervals results in the lower and upper fuzzy models. The expected covariance of the residuals between the observed data and the local model output is given as follows:

$$\Delta \hat{y}_j = cov(y_j - \hat{y}_j) = \hat{\sigma}_j^2 I + \hat{\sigma}_j^2 \psi_j^T (\psi_j \psi_j^T)^{-1} \psi_j, \quad (16)$$

where  $y_j$  is the output of the local model  $j$ , and the variance of the local noise signal is  $E\{e_j e_j^T\} = \hat{\sigma}_j^2 I$ . The upper and lower fuzzy model interval functions of the local linear model are defined as follows:

$$\bar{f}_j(z_i(k)) = \psi_{i,j}^T \theta_j + \bar{\alpha} \hat{\sigma}_j \left( 1 + \psi_{i,j}^T (\psi_j \psi_j^T)^{-1} \psi_{i,j} \right)^{1/2} \quad (17)$$

$$\underline{f}_j(z_i(k)) = \psi_{i,j}^T \theta_j + \underline{\alpha} \hat{\sigma}_j \left( 1 + \psi_{i,j}^T (\psi_j \psi_j^T)^{-1} \psi_{i,j} \right)^{1/2}, \quad (18)$$

where  $i=1, \dots, N$  is a set of data samples,  $\bar{\alpha}$  and  $\underline{\alpha}$  are the parameters of the fuzzy confidence intervals that should be tuned to obtain a certain confidence probability. The confidence probability is defined as:

$$CP = \frac{\sum_{i=1}^N \delta_i}{N}, \quad (19)$$

where  $N$  is the number of the data set and  $\delta_i$  are binary variables that indicate whether the sample data  $Z_i$  belong to the interval.

The objective of the fuzzy interval is to obtain the upper and lower functions as narrowly as possible while the interval contains the greatest possible amount of measured data. Specifically, confidence probability and its normalized average width are used to evaluate the performance of the fuzzy interval model. The Normalized Average Width (NAW) is defined as:

$$NAW = \frac{1}{N \cdot (y_{\max} - y_{\min})} \sum_{i=1}^N \bar{f}_i - \underline{f}_i, \quad (20)$$

where  $N$  is the size of the data set,  $y_{\max}$  and  $y_{\min}$  are the maximum and minimum values of measurement, and  $\bar{f}_i$  and  $\underline{f}_i$  are the upper and lower bounds of the fuzzy interval.

### C. Proposed Method

The optimization software "HOMER" for distributed power systems is used for the planning of the MG of the case study. This software allows the evaluation of different configurations of energy systems [25]. Via a simulation process, the optimization algorithms of HOMER determine the best configuration for a particular hybrid system based on the balance of power, technology options, costs, the specification of the components, and the available resources of the community [26].

Different scenarios were simulated in this study to analyze the feasibility of the implementation of the MG. The power balance in Eq. (2) is modified according to the scenarios generated, and the planning problem is solved for each scenario. Simulation scenarios are based on the fuzzy confidence interval models of both solar irradiance and wind speed, which, for all cases, are tuned at 90% of the confidence level. When the best and worst cases for the resources are considered, the power output of the resources are modified (see Eq. (3) and Eq. (4)) according to the lower and upper bounds of the fuzzy interval.

The baseline scenario corresponds to annual measured profiles of the solar irradiation and wind speed. A scenario with the worst case of the wind resource is considered, in which the wind speed equals the lower bound of the fuzzy interval. A scenario with the worst case of both the wind and the solar resources is also considered; both resources equal their corresponding lower bound of the fuzzy interval. Finally, a scenario with the best case of the wind resource is presented, in which the wind speed is estimated to be the upper bound of the fuzzy interval. The last step in this method corresponds to selecting the final design of the MG. This configuration is chosen based on the most suitable technical-economic and environmental criteria for the implementation of the project.

## III. CASE STUDY

The case study is located at the geographic coordinates 38.54°S; 73.50°W, which correspond to the indigenous Mapuche community of José Painecura, Hueñalihuen, located in Carahue, in the IX Region (Araucanía) in Chile. The community is connected to the main network, however, the

quality of the service is poor, with many unscheduled outages each year.

### A. Load Community

First in the MG planning, it is necessary to estimate the energy demand of the community accurately. This is an important step that will help in determining the optimal sizes of the different equipment and their components. For an initial estimation of the load profile, we use real-life measurements first together with a social survey of another community in the same region, as is shown in Fig. 1. This community is located 54 km southeast of the José Painecura community. Its main productive activity is agriculture for subsistence, and raising small livestock. Due to their geographic proximity, their similar electrical equipment characteristics, their similar productive activities, and, most importantly, the same identification as Mapuche ethnic groups, we have assumed a close similarity between the electric consumption behavior and activities of the two communities [27], [28].

For the approximated load profile per month in the José Painecura community, the profile presented in Fig. 1 was scaled as a function of the estimated total energy demand (which was provided by the local electricity distributor). Measurements from only 7 homes are available, so we used bimonthly consumption readings from these houses in the year 2014, and have included 36 more houses from the surrounding area, from the town of Hueñalihuen in which the José Painecura community is located. The estimated electricity demand is 65.4 [kWh/day], with an average of 2.72 [kW], a power peak of 9.75 [kW], and a load factor of 0.29.

Next, the analysis of the existing solar and wind resources in the area was done to determine the annual profiles of the renewable energy at the location. Empirical measurements of weather variables were combined with simulated information to fill the incomplete information. The models are mesoscale, called "Explorador Solar" (Solar Explorer) [29] and "Explorador Eólico" (Wind Explorer) [30] from the Department of Geophysics of the University of Chile.

### B. Fuzzy Interval for the Solar Resource

Measurements of the horizontal solar irradiation were recorded for a period of 94 consecutive days. The database of the "Explorador Solar" was used to fill in incomplete information. Fig. 2 shows the daily insolation throughout the whole year. The average annual insolation is 4.3 [kWh/m<sup>2</sup>]. This resource has a strong seasonal dependence, i.e. less during the winter period, and with the presence of clouds, with around 30% of solar resource uncertainty.

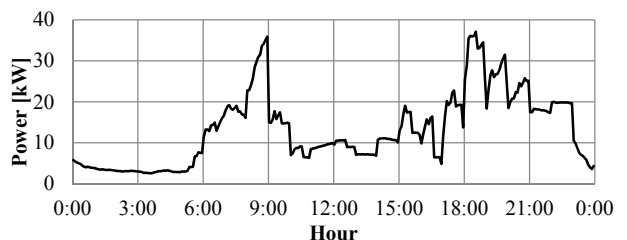


Fig. 1. Estimated Load Profile of the Community [31].

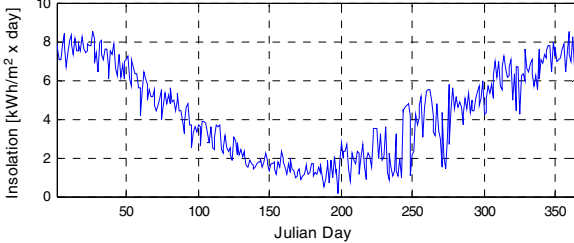


Fig. 2. Average Insolation.

The Global Horizontal Irradiance model was obtained based on the T&S model presented in Section II.B. The annual solar data was divided into 60% for training, 20% for testing, and 20% for validation. In total, 10 regressors and 4 rules were obtained. For the model evaluation, the root-mean-squared errors (RMSE) and the mean-absolute errors (MAE) were used. The RMSE and MAE are 0.0510 [ $\text{kWh}/\text{m}^2$ ] and 0.0353 [ $\text{kWh}/\text{m}^2$ ] for the training data, 0.0687 [ $\text{kWh}/\text{m}^2$ ] and 0.0429 [ $\text{kWh}/\text{m}^2$ ] for the test data, and 0.0583 [ $\text{kWh}/\text{m}^2$ ] and 0.0416 [ $\text{kWh}/\text{m}^2$ ] for the validation data set. Subsequently, the covariance method presented in Section II.B was used, to characterize the uncertainty of the solar resource, with a confidence level of 90%. The fuzzy intervals using 120 hours are presented in Fig. 3 as the validation data set. In the validation data set the CP is 86.91% and the normalized average width (NAW) is 14.43%; i.e., less than 15% of the measured data are outside the interval, which is a reasonable representation of the uncertainty for the application.

### C. Fuzzy Interval for Wind Resource

The data of the average wind speed and direction were measured in a weather station at the height of 5 [m]. This data was extrapolated to 15 [m], which is the approximate height of a wind turbine used for small-scale generation. The data include a period of 94 days, and the yearly information was completed using the database of the “Explorador Eólico”.

Fig. 4 shows the annual cycle of wind speed. The wind speed is 5 [m/s] on average, with speeds between 2 [m/s] and 6 [m/s] nearly 50% of the time. Over 75% of the time, wind speed reaches above the level of 3 [m/s] that corresponds to the starting speed of a typical wind turbine which allows breaking the inertia of the blades. Furthermore, less than 5% of the time, the wind speed can be over 12 [m/s], which is the threshold for the safe operation of such equipment. The seasonal dependence is strong, with greater wind resources during the winter period, which is also the period with the lowest solar irradiation.

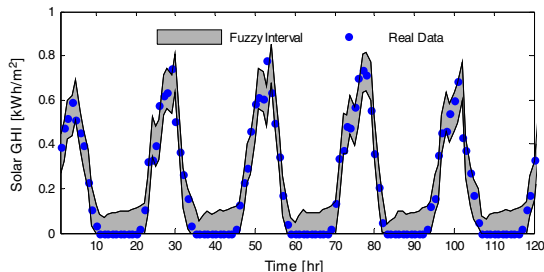


Fig. 3. Measured Solar Global Horizontal Irradiance and the Fuzzy Interval Model.

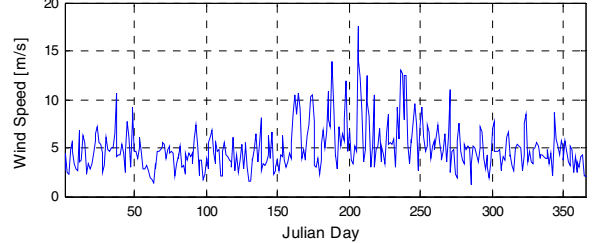


Fig. 4. Average Wind Speed.

The wind speed model was obtained based on the T&S model presented in Section II.B, and modelled in the same way as the solar resource. A model with 1 regressor and 2 rules was derived. The RMSE and MAE of the estimated wind speed are 1.0432 [m/s] and 0.7005 [m/s] for the training data set, 1.3258 [m/s] and 0.9553 [m/s] for the test data set, and 0.8443 [m/s] and 0.5979 [m/s] for the validation data set. The fuzzy interval for the wind speed is shown in Fig. 5, using 120 hours as the validation data set. In the validation data set, the CP equals 93.66% and the NAW is 24.27%. This means that less than 8% of the measured data is outside the narrowest range that covers the interval model, which is adequate for the application.

## IV. MICROGRID PLANNING FOR THE CASE STUDY

### A. Components

For the assessment technical and economic details of the following components were considered: Amerisolar AS-6P30 of 250 [W] photovoltaics arrays, hereafter named “PV”; wind turbine Osiris 10 of 10 [KW] and Ouyad 4.0-3000 of 3 [KW], hereafter named “A10” and “A3”, respectively; bidirectional converter AC/DC Victron Multiplus of 5 [KW], hereafter named “AC/DC”; batteries Luxcel 12V 100AH, hereafter named “Bat”; and a genset Kipor KDE60SS3 of 40 [KW], hereafter named “GS”.

Both the high terrain and the surface roughness of the power law were obtained by comparing wind speed to 5 [m] and 15 [m], based on the “Explorador Eólico”; an inflation rate of 3.1% corresponds to the median for September of the last ten years. A discount rate of 10% and evaluation horizon of 20 years was established. The diesel price was estimated at 0.64 [\$/l], based on public information delivered by the National Energy Commission of Chile. The purchase price of energy corresponds to the rate in October that a residential customer usually pays, and the selling price of energy was valued at the node price of the closer energy bar (the transmission system).

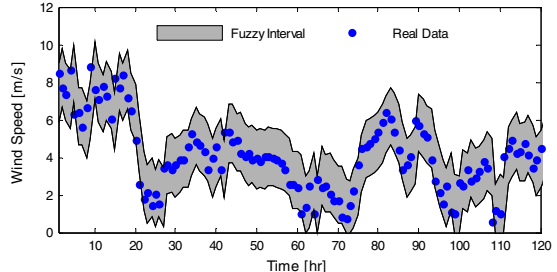


Fig. 5. Measured Wind Speed and the Fuzzy Interval Model.

Finally, the unscheduled outages are quantified using information that was delivered by a local distributor in 2014. In a total of 43 faults per year, with a time repair average of 9 [hrs], and a variability of 107% were identified.

The investment, operation, and maintenance cost of the technologies to assess are presented in TABLE I. The investment costs include both equipment costs and costs associated with installation and project management. The final cost includes the work of the engineers, technicians, and drafters, among others. In addition, the costs of transport of personnel and RRHH logistics that allow the assembly, installation, and commissioning of the system are included.

Also considered are the equipment transport from the port to the destination, and the local transportation; taxes, mainly Value Added Tax (VAT) corresponding to 19% of the investment; and reserve funds for emerging costs, spare parts, emergencies, inconveniences, and natural disasters are also included. For simplicity, it is assumed that the replacement cost is equal to the investment cost.

The wind turbines have strong economies of scale in the costs per kilowatt, which vary significantly based on the power rating. The installation and project management cost are estimated as 18% and 6% of the value of the equipment, respectively, considering the split cost presented for the IEA in [32]. The cost for the spare parts is considered to be 10% of the cost of the equipment and installation; and the contingency cost is estimated as 15% approximately of the total value of the equipment, installation, project management, and transportation [33].

The photovoltaic system has a lower investment cost per kilowatt than the wind turbines. The installation cost is calculated including the lease of a car and the work of an electrician and one helper, valuing the professional hour at 1 UF, a Chilean currency equivalent to 37 [\$/hr]. The transport of the equipment per kilogram is estimated to be 75% of the price of moving the turbines, due to the modularity of the photovoltaic array [33].

TABLE I.  
ESTIMATED INSTALLATION, OPERATION, AND MAINTENANCE COSTS.

Capital Expense	A10	A3	PV	Bat	AC/DC	GE
	\$/kW	\$/kW	\$/kW	\$/kWh	\$/kW	\$/kW
Equipment	5169	9973	1248	156	539	242
Installation	734	1795	1364	36	0	34
Project Management	245	598	75	0	0	15
Transport	3009	1839	1966	777	201	11
Spare parts	590	1177	261	19	54	28
Contingency	1373	2131	698	145	111	45
Tax	2113	3328	1066	215	172	71
<b>Total</b>	<b>13233</b>	<b>20841</b>	<b>6679</b>	<b>1349</b>	<b>1076</b>	<b>445</b>
	\$/kW /yr	\$/kW /yr	\$/kW /yr	\$/kWh /yr	\$/kW /yr	\$/kW /yr
O&M Cost	198	313	12	0	5	85 <sup>a</sup>

The costs of project management, spare parts, and contingency are estimated in a way similar to that of the installation of the wind turbines. The costs for the genset, battery bank, and bidirectional converter are similarly estimated, except that the latter does not include costs of project management, because those may be included in the installation of the photovoltaic system and/or wind turbine.

Finally, fixed costs of the project are considered. They include construction of a house of 20 [m] to protect the genset from climate conditions, and a stand of 16 [m] to protect the bank of batteries, with costs of \$12,133 and \$10,703, respectively. It is expected to have subsidized financing from public funds of \$145,600, which has been included in the economic estimate.

For PV cost analysis, the cost of the charger controller and the aluminium structure is included; the O&M cost is low and corresponds to an annual investment of 1% which includes the PV cleaning, and the degradation of structural elements, among others [34]. The same consideration is also given to the converter as a part of the photovoltaic system. The wind turbine investment cost includes the generator, blades, tower, controller, and inverter protections, and the maintenance costs correspond to 2% of the annual cost of the investment [35]. The diesel requires maintenance every 250 hours of operation. The lead-acid batteries are sealed and are maintenance free.

Note that the investment, operation, and maintenance costs are estimated values which might be underestimated in regard to the effective cost of the proposed microgrid to be installed because other expenses are not analysed in this work. However, from the results presented, the microgrid sizing is obtained under these assumptions.

## B. Results

Using the technical and economic data described in Section IV.A, several topologies of PV/wind/diesel/battery with different capacities and under different scenarios obtained from the fuzzy intervals presented in Section II.B are simulated in HOMER. The HOMER software determines the optimal configuration within the feasible solutions according to the objective function and constraints presented in Section II.A. The selection criteria of the system configuration of the microgrid correspond to the maximization of the energy generated by renewable resources, without higher cost than the current rate. The results are presented in TABLE II.

According to the results, the main difference in the design of microgrids is the sizing of the wind turbines. Also, due to the high cost of this equipment, installing a wind turbine with lower capacity can be considered if the wind resource conditions are less favorable (worst case) than those estimated in the base case. Similarly, if the wind conditions are underestimated in the base case, an additional wind turbine installation will be required (WT 3 [kW]).

On the other hand, according to the results obtained in Section III, the fuzzy interval width of the solar resource is 10% narrower than the wind resource width, which indicates less uncertainty associated with the solar resource, as we

expected, and therefore the pattern of solar irradiation is more predictable. Because of this, the same PV array 3 [kW] is considered for both scenarios (the Best and Worst cases). Additionally, increased wind turbine generation (Best Case) could be considered for the most favorable scenarios for available renewable resources with, consequently, a lower use of a diesel generator. Due to the particular conditions of the location we studied, where the wind resource is stronger but with high uncertainty, the design of the microgrid will depend heavily on the conditions of this resource.

Using a conservative approach, a less risky approach for the investment is considered; that is the microgrid design obtained for the worst case (lesser wind and solar resources) is evaluated. In this scenario, an annual energy of 3315 [kWh/year] is produced with an A3 wind turbine, corresponding to 13.17% of the total energy, a PV contribution of 12.51% (3148 [kWh/year]); a 9.35% contribution of diesel generation (2352 [kWh/year]), and a 64.97% main grid contribution (16349 [kWh/year]).

Fig. 6 presents a summary of the net present cost of the designed microgrid using the worst case for wind and solar generation. Fig. 7 shows the monthly contribution of each power generating unit. 64% and 21% of the investment are the costs of wind turbine A3 and PV, respectively. According to a scenario analysis, at least 24% of the energy at the operation cost of the microgrid system (considering replacement, maintenance, and fuel costs) corresponds to 16% of the total cost.

The greatest contribution of wind turbine A3, close to 1 [kW], occurs in the winter. On the other hand, PV presents contributions of around 0.5 [kW] in the summer season. Finally, the diesel generator, besides supplying the load under failures of mains, constitutes approximately 20% of the required power in the autumn, when the availability of solar and wind resources is reduced. Note that the net present cost of the selected topology is \$ 186,374 which could be financed in part by public funds and permits at least an estimated 24% annual renewable generation.

## V. CONCLUSIONS

Various scenarios for planning a microgrid connected to the main grid in the rural Mapuche community of José Painecura were analyzed in this work. The scenarios were generated using fuzzy interval models for the solar and wind renewable resources.

The fuzzy interval models allowed characterizing the renewable resources with a band that contains the measurement values at a certain confidence level. According to the resulting fuzzy intervals, the wind resource presented a higher uncertainty than the solar resource. The different scenarios of renewable resources were also defined from the fuzzy intervals and used for the planning stage.

TABLE II. MICROGRID CONFIGURATION UNDER DIFFERENT SCENARIOS.

	Unit	Base Case	Worst Case Wind Speed	Worst Case Wind Speed & Solar GHI	Best Case Wind Speed
<b>Configuration</b>					
A10	[unit]	1	0	0	1
A3	[unit]	0	1	1	1
PV	[kW]	3.00	3.00	3.00	3.00
Bat	[unit]	5	5	5	5
AC/DC	[kW]	3.00	3.00	3.00	3.00
GS	[kW]	10.00	10.00	10.00	10.00
<b>Operation</b>					
Renewable fraction	[%]	69	27	24	90
Hours of Diesel Gen. operation	[hr/yr]	300	482	509	176
Fuel used by Genset, GS	[l/year]	427	762	810	236

Based on the scenarios generated, and considering technical-economic-environmental criteria, the appropriate microgrid topologies for implementation can be defined for a decision maker. An appropriate topology for a microgrid is obtained from the resulting planning using the worst case scenario of both diminished wind and solar resources. Also, compared to the other scenarios, the microgrid topology is very similar, but the investment risk is minimized under this worst case scenario.

For further research, we consider that a multiobjective optimization approach can be used to extend the analysis, including environmental and social impact in the objective function.

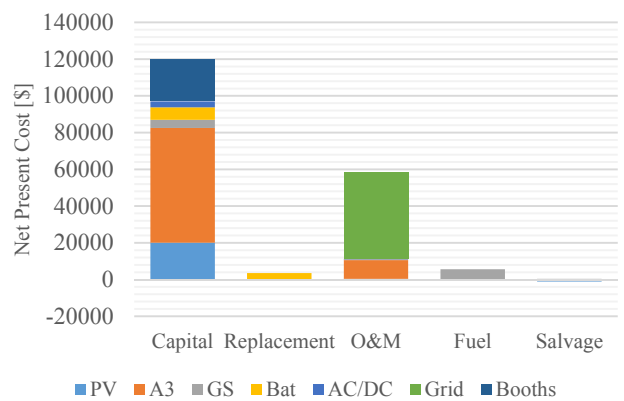


Fig. 6. Cost of the Designed Microgrid under the Worst Case (of wind and solar resources).

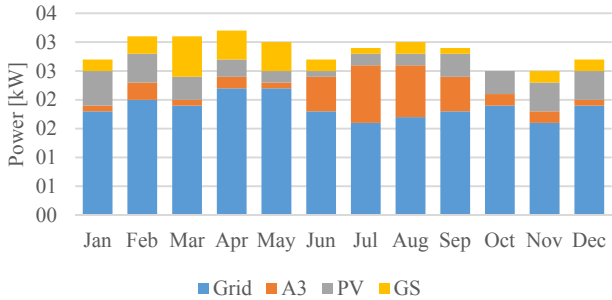


Fig. 7. Monthly Power for the Microgrid under the Worst Case (of wind and solar resources)

## ACKNOWLEDGMENTS

This work has been partially supported by the Millennium Institute “Complex Engineering Systems” (ICM: P-05-004- F, CONICYT: FBO16); by the Solar Energy Research Center SERC-Chile, CONICYT/FONDAP/15110019; and by the FONDECYT Project 1140775. Luis G. Marín has been supported by a Ph.D scholarship from CONICYT-PCHA/Doctorado Nacional para extranjeros/2014-63140093

## REFERENCES

- [1] M. G. Pereira, M. A. V. Freitas, and N. F. da Silva, “Rural electrification and energy poverty: Empirical evidences from Brazil,” *Renew. Sustain. Energy Rev.*, vol. 14, no. 4, pp. 1229–1240, 2010.
- [2] L. Ferrer-Martí, A. Garwood, J. Chiroque, B. Ramirez, O. Marcelo, M. Garfi, and E. Velo, “Evaluating and comparing three community small-scale wind electrification projects,” *Renew. Sustain. Energy Rev.*, vol. 16, no. 7, pp. 5379–5390, 2012.
- [3] E. Baldwin, J. N. Brass, S. Carley, and L. M. MacLean, “Electrification and rural development: issues of scale in distributed generation,” *Wiley Interdiscip. Rev. Energy Environ.*, vol. 4, no. 2, pp. 196–211, 2015.
- [4] K. Ubilla, G. A. Jimenez-Estevez, R. Hernandez, L. Reyes-Chamorro, C. Hernandez Irigoyen, B. Severino, and R. Palma-Behnke, “Smart microgrids as a solution for rural electrification: Ensuring long-term sustainability through cadastre and business models,” *IEEE Trans. Sustain. Energy*, vol. 5, no. 4, pp. 1310–1318, 2014.
- [5] J. Leary, A. While, and R. Howell, “Locally manufactured wind power technology for sustainable rural electrification,” *Energy Policy*, vol. 43, pp. 173–183, Apr. 2012.
- [6] R. H. Lasseter, “MicroGrids,” in *Power Engineering Society Winter Meeting, 2002. IEEE*, 2002, vol. 1, pp. 305–308.
- [7] T. E. Del Carpio Huayllas, D. S. Ramos, and R. L. Vasquez-Arnez, “Microgrid systems: Current status and challenges,” in *Transmission and Distribution Conference and Exposition: Latin America (T-D-LA), 2010 IEEE/PES*, 2010, pp. 7–12.
- [8] X. Vallvé, “Micro-grid power systems based on renewable energy for rural electrification: benefits, examples and steps to promote these solutions,” in *International hearing on Climate Change an Energy access for the poor*, 2010, pp. 26–28.
- [9] J. Agredano, J. Huacuz, and G. Munguía, “La electrificación de Puerto Alcatraz, Baja California Sur, México, Un análisis retrospectivo.” 2007.
- [10] A. Khodaei and S. Bahramirad, “Microgrid planning under uncertainty,” *IEEE Trans. Power Syst.*, vol. 30, no. 5, pp. 1–9, 2015.
- [11] A. Khodaei, “Provisional Microgrid Planning,” *IEEE Trans. Smart Grid*, pp. 1–9, 2015.
- [12] B. Hong, L. Guo, B. Jiao, W. Liu, and C. Wang, “Multi-objective stochastic optimal planning method for stand-alone microgrid system,” *IET Gener. Transm. Distrib.*, vol. 8, no. 7, pp. 1263–1273, 2014.
- [13] H. K. Alfares and M. Nazeeruddin, “Electric load forecasting: Literature survey and classification of methods,” *Int. J. Syst. Sci.*, vol. 33, no. 1, pp. 23–34, Jan. 2002.
- [14] A. Ghanbari, E. Hadavandi, and S. Abbasian-Naghneh, “Comparison of artificial intelligence based techniques for short term load forecasting,” in *2010 Third International Conference on Business Intelligence and Financial Engineering*, 2010, pp. 6–10.
- [15] S. Jafarzadeh, M. S. Fadali, and S. Member, “Solar power prediction using interval type-2 TSK modeling,” *IEEE Trans. Sustain. Energy*, vol. 4, no. 2, pp. 333–339, 2013.
- [16] J. Xia, P. Zhao, and Y. Dai, “Neuro-fuzzy networks for short-term wind power forecasting,” in *2010 International Conference on Power System Technology*, 2010, pp. 1–5.
- [17] A. Khosravi, S. Nahavandi, S. Member, and D. Creighton, “Construction of optimal prediction intervals for load forecasting problems,” *IEEE Trans. Power Syst.*, vol. 25, no. 3, pp. 1496–1503, 2010.
- [18] H. Quan, D. Srinivasan, and A. Khosravi, “Short-term load and wind power forecasting using neural network-based prediction intervals,” *IEEE Trans. Neural Learn. Syst.*, vol. 25, no. 2, pp. 303–315, 2014.
- [19] D. Saez, F. Avila, D. Olivares, C. Canizares, and L. Marin, “Fuzzy Prediction Interval Models for Forecasting Renewable Resources and Loads in Microgrids,” *IEEE Trans. Smart Grid*, vol. 6, no. 2, pp. 548–556, 2015.
- [20] F. Veltman, L. G. Marin, D. Saez, L. Gutierrez, and A. Nuñez, “Prediction interval modelling tuned by an improved teaching learning algorithm applied to load forecasting in microgrids,” in *2015 IEEE Symposium Series on Computational Intelligence*, 2015, pp. 651–658.
- [21] W. Su, Z. Yuan, and M. Y. Chow, “Microgrid planning and operation: Solar energy and wind energy,” in *IEEE PES General Meeting, PES 2010*, 2010, pp. 1–7.
- [22] T. Takagi and M. Sugeno, “Fuzzy identification of systems and its applications to modeling and control,” *Syst. Man Cybern. IEEE Trans.*, vol. SMC-15, no. 1, pp. 116–132, 1985.
- [23] I. Škrjanc, “Fuzzy confidence interval for pH titration curve,” *Appl. Math. Model.*, vol. 35, no. 8, pp. 4083–4090, Aug. 2011.
- [24] R. Babuška, *Fuzzy Modeling for Control*. Springer Netherlands, 1998.
- [25] NREL National Renewable Energy Laboratory, “Getting Started Guide for HOMER Version 2.1.” Golden, Colorado, p. 30, 2005.
- [26] M. Kolhe, K. M. I. U. Ranaweera, and A. G. B. S. Gunawardana, “Techno-economic optimum sizing of hybrid renewable energy system,” in *Industrial Electronics Society, IECON 2013 - 39th Annual Conference of the IEEE*, 2013, pp. 1898–1903.
- [27] P. Kadurek, W. L. Kling, P. F. Ribeiro, and J. F. G. Cobben, “Electricity demand characterization for analyzing residential LV distribution networks,” in *PowerTech (POWERTECH), 2013 IEEE Grenoble*, 2013, pp. 1–5.
- [28] A. Cagni, E. Carpaneto, G. Chicco, and R. Napoli, “Characterisation of the aggregated load patterns for extraurban residential customer groups,” in *Electrotechnical Conference, 2004. MELECON 2004. Proceedings of the 12th IEEE Mediterranean*, 2004, vol. 3, pp. 951–954 Vol.3.
- [29] A. Molina and R. Rondanelli, “Explorador de Energía Solar,” 2012. [Online]. Available: <http://walker.dgf.uchile.cl/Explorador/Solar2/>.
- [30] Departamento de Geofísica, “Explorador de Energía Eólica,” 2012. [Online]. Available: <http://walker.dgf.uchile.cl/Explorador/Eolico2/>.
- [31] V. Caquilpan, “Estimación de la demanda eléctrica y potencial energético de recursos renovables para el diseño de micro-redes en comunidades rurales,” Universidad de Chile, 2016.
- [32] L. M. Moore and H. N. Post, “Wind Energy and Electricity Prices - Exploring the ‘merit order effect.’” European Wind Energy Association, Brussels, Belgium, p. 38, 2010.
- [33] M. Arriaga, C. A. Canizares, and M. Kazerani, “Renewable Energy Alternatives for Remote Communities in Northern Ontario, Canada,” *Sustain. Energy, IEEE Trans.*, vol. 4, no. 3, pp. 661–670, 2013.
- [34] C. Breyer, A. Gerlach, J. Mueller, H. Behacker, and A. Milner, “Grid-parity analysis for EU and US regions and market segments - Dynamics of grid-parity and dependence on solar irradiance, local electricity prices and PV progress ratio,” in *European Photovoltaic Solar Energy Conference*, 2009, no. 24th, pp. 4492–4500.
- [35] Bornay Aerogeneradores, “Aerogenerador Bornay 3000,” Castalla, España, 2011.